

Morphological and Humidity Sensing Studies of Pure WO₃

N.K. Pandey and Sanchita Singh
(Sensors and Materials Research Laboratory,
Department of Physics, University of Lucknow,
Lucknow, 226007, U.P., India)

Abstract: Present paper deals with a sensing performance of pure WO₃ at different annealing temperatures, the sensing properties and characterization of pure WO₃. Pure WO₃ have been prepared through solid state reaction route. These samples have been annealed at temperature (300°C-600°C) for three hours and then exposed to humidity chamber. At 600°C temperature we find out the highest sensitivity of WO₃ which is 10.40 MΩ/RH%. As calculated from Scherer's formula crystallite size for the sensing elements of pure WO₃ is 72.4 nm. Structural properties studied by X-Ray diffraction method. SEM micrograph reveal that as the temperature increases the porosity of materials increases forming clusters for WO₃. This feature shows the adsorption and condensation of waters vapours. Now the grain size of pure WO₃ at annealing temperatures 300°C, 400°C, 500°C and 600°C are 114nm, 135nm, 148nm and 158 nm respectively. The pressed powder pellets have been annealed in air at temp.300°C to 600°C for 3hours and checked for its sensing efficiency. Each heat treated pellet was exposed to humidity under controlled condition and variations in resistance with the humidity were recorded.

Keywords: Sensitivity, Humidity, Nanostructures, Resistance and Surface Morphology.

Date of Submission: 15-08-2019

Date of Acceptance: 30-08-2019

I. Introduction

Sensors are key elements in the rapidly evolving fields of measurements, instrumentations and automated systems. In this paper we prepare the humidity sensor by materials. Humidity is a permanent environmental factor. Humidity is the amount of water vapour in the air. In this paper we prepare the metal oxide ceramic humidity sensor. Metal oxide ceramic humidity sensors based on porous and sintered. Oxides have attracted much attention due to their chemical and physical stability. Research has been going onto find suitable materials that show good sensitivity over large range of relative humidity (RH), low hysteresis and properties that are stable. Among the metallic oxide, tungsten oxide (WO₃) has many technological applications. It is good electrochromic, optochromic and gasochromic material. WO₃ behave like n-type semiconductor. WO₃ is an important kind of wide bandgap, semiconducting metal oxides. Aihua yan et al. have synthesized WO₃ nanowall using solvothermal(1). Su et al. prepared WO₃ thick film using screen printing method(2). Z hou et al. highly ordered mesoporous tungsten oxide have been synthesized via the hard templating method(3). Liu et al. have synthesized tungsten oxide nanorods assembled microspheres by a facile hydrothermal process(4). Metal oxide semiconductor (WO₃) have attracted significant attention towards gas sensing and humidity sensing due to their simple implementation, low cost and good reliability for real time control system with respect to other sensors. In ceramic oxide water molecules are adsorbed to increase the conductivity of n-type ceramics and to decrease the conductivity of p-type ceramics, because the conductivity is related to the no of free electrons of surface. This type of sensing is called "electronic type"

Now we trace the sensitivity of semiconductor. We have reported characterization and humidity sensing studies of (pure) WO₃ prepared by solid state reaction route and also show the characterization for WO₃ at 600°C annealing temp. by XRD and SEM.

Preparation of sample and experimental details

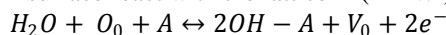
first of all we prepare samples of pure WO₃ by solid state reaction route. The materials WO₃ (Loba Chemie, 99.99%). Now take a wo₃, 5wt% polyvinyle alcohol (pva) has been added as a binder because it increases the strength of materials. The powder have been mixed uniformly and made fine by grinding in mortar with pestle for 3hours. The resultant powder have been pressed into pellet shape by uniaxially applying pressure of 250 Mpa in a hydraulic press machine (M.B. Instruments, Delhi, India) at room temp. The pellet samples prepared are in disc shape having diameter of 12 mm and thickness 2mm. The pressed powder pellets have been annealed in air at temp.300°C to 600°C for 3h in an electric muffle furnace (Ambassador, India). After sintering, samples have been exposed to humidity in a specially designed humidity control chamber. Inside the humidity chamber,

a thermometer (+_1°C) and standard hygrometer (digital, +_1%RH) are placed for the purpose of calibration. Variation in a resistance has been recorded with change in % RH. When resistance gets increases then relative humidity decreases at different temperatures. Variation in resistance of the pellet has been recorded by a multifunctional digital multimeter (±0.001 MΩ.VC⁻). Copper electrode has been used to measure the resistance of the pellet. The resistance of the pellet has been measured normal to the cylindrical surface of the pellet. We use the K₂SO₄ solution as a humidifier and KOH sol. as dehumidifier. To see the effect of ageing, the sensing properties of these elements have been examined again in the humidity control chamber after six months. In this paper pure wo₃ indicated by “W”. This experimental work shown by fig(1).

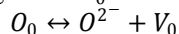
Principle of operation of WO₃

The mechanism of interaction of water vapour molecules with a porous metal oxide. It is proposed that the water vapour chemisorbs on the surface of metal oxide to form hydroxyl groups. The hydroxyl group with an adjacent surface -2 ion. The adsorption of water molecules on the surface takes place via a dissociative chemisorptions process which may be described in a two step process a given below.

1-water molecules adsorbed on grain surface react with the lattice A (A→W) as



Where O₀ represent the lattice oxygen and V₀ is the vacancy created at the oxygen site according to the reaction



2-Doubly ionised oxygen , displaced from the lattice ,reacts with the H+ coming from the dissociation of water molecules to form a hydroxyl group as given below

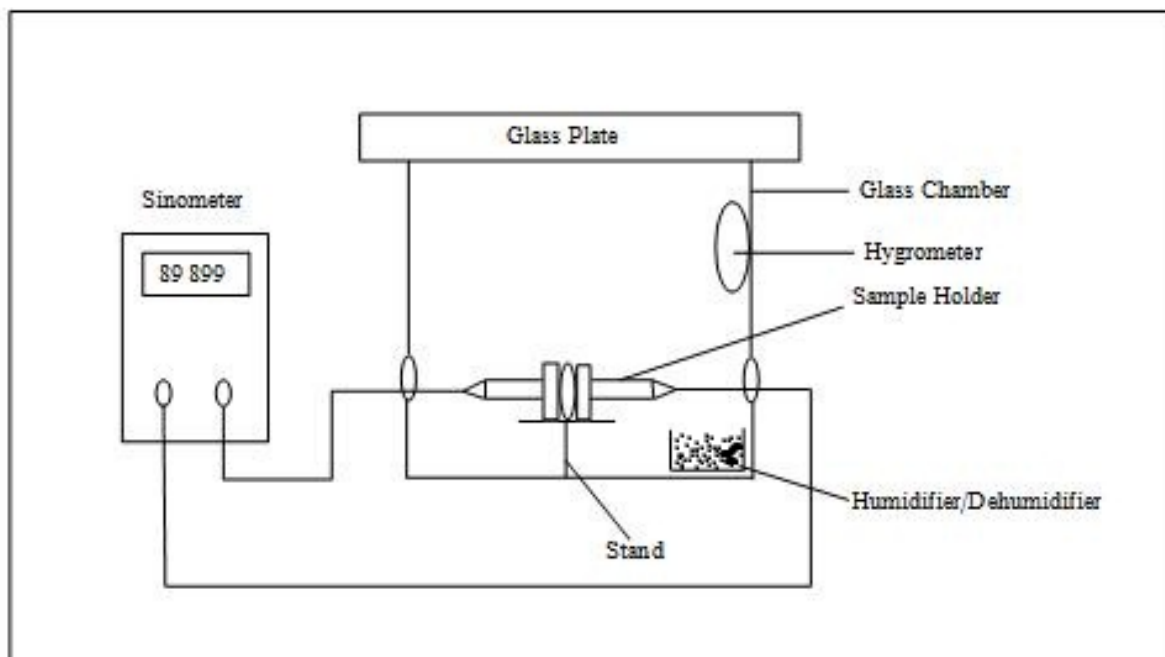
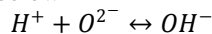


Fig.01: Systematic diagram of humidity sensing apparatus.

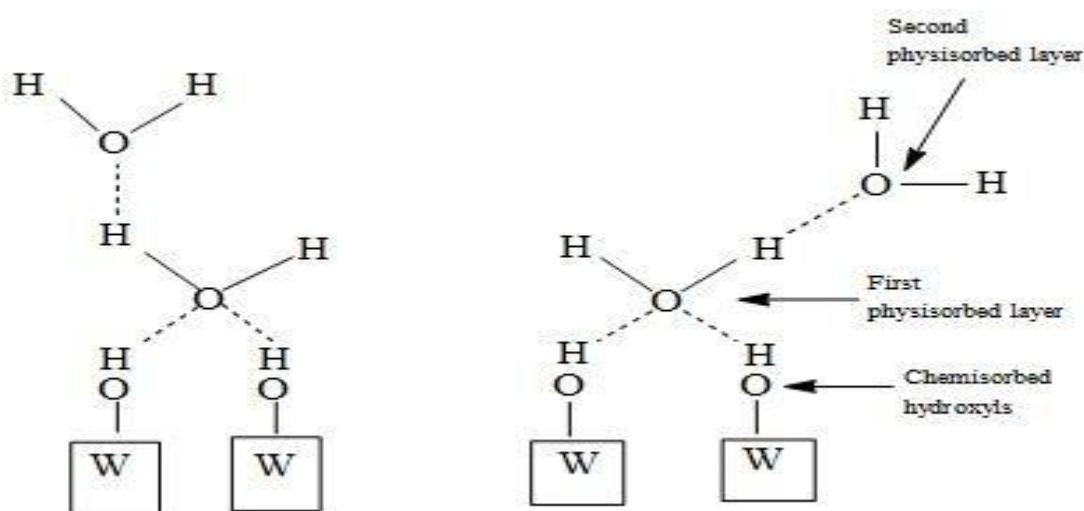


Fig.02; Sensing Mechanism of solid state humidity sensor

II. Result and discussion

Table 01: Sensitivity of pure wo₃

Annealing Temp. °C	a		b		C	
	10-50	50-99	10-50	50-99	10-50	50-99
300°C	14.8	1.79	15.14	1.32	13.32	1.57
400°C	17.72	1.59	17.87	1.32	15.87	1.12
500°C	14.36	2.95	18.75	2.00	19.77	2.00
600°C	17.42	4.67	18.25	4.06	14.97	3.89

a = Increasing cycle of relative humidity, b= Decreasing cycle of relative humidity, c = increasing cycle of relative humidity (after six months)

Table 02:

Sensitivity of sample (MΩ%RH) in the 10-99% RH range			
Annealing Temp. °C	a	b	c
300°C	7.64	7.52	6.85
400°C	8.84	8.76	7.75
500°C	9.53	9.52	9.98
600°C	10.4.	10.43	8.87

1-Humidification graph: In fig.(03) variation in resistance with the change in relative humidity has been recorded for the sensing elements of pure WO₃ at annealing temp.300°C-600°C. All the results have been found to be repeatable. There is continuous decrease in the value of resistance with increase in the %RH for the samples pure wo₃ at annealing temp 600°C are showing higher values of sensitivity. Fig(3) shows large decrease in the value of resistance for the initial value of relative humidity from 10%- 50%RH while in 50%-99%RHrange the fall in resistance is slow and for both range the sensitivity of W are17.42MΩ/%RH and 4.67MΩ/%RH-respectively. In the n-type semiconductor at high humidity condition(>50%RH)and low humidity condition (<50%RH).Because for the low humidity condition electrons may be trapped by the surface defect are released when the water molecules are co-adsorbed onto the surface causing the some of the oxygen ions to be desorbed and relatively high resistance at low humidity is maintained . At high humidity condition (>50%RH) the electrons may be trapped by the surface defects such as ionised oxygen vacancies and that these may be released when water molecules are adsorbed onto the defect sites and therefore resulting in reduce of the value of resistance at high humidity.

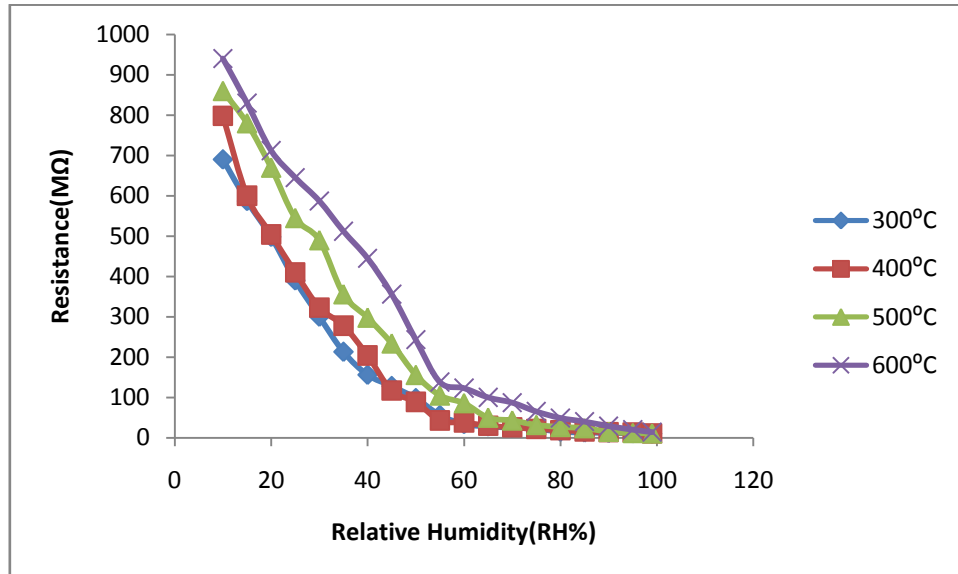


Fig.03: Variations in Resistance with % RH for Sample Pure WO_3 annealing temperature at 300°C to 600°C (Humidification graph)

2-Sensitivity comparison graph: Fig.(04) is the sensitivity graph for pure WO_3 (W) at (300°C-600°C) for the range 10% to 99% RH. The sensitivity of pure WO_3 increases with increase of annealing temperature at 600°C. Pure WO_3 shows highest value of sensitivity at 600°C. The average sensitivity for range 10% to 99% RH for pure WO_3 is 10.40 $M\Omega/\%RH$ at annealing temperature 600°C. Which is shown in table 2. The sensitivity of all samples at annealing temperatures 300 to 600°C increases when the temperatures gets increases.

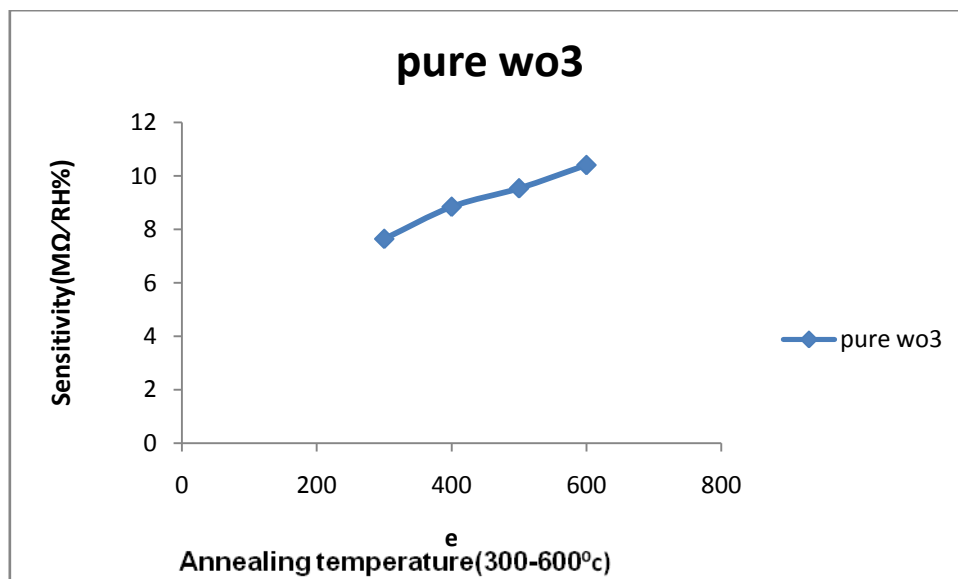


Fig.04: Sensitivity graph for Humidification cycle

3-Hysteresis graph: Fig (5),(6),(7), and (8) shows the hysteresis graphs for WO_3 at annealing temp. 300 to 600°C. The phenomenon hysteresis may be understood in the manners that due to the adsorption of water on the surface of the sensing elements a chemisorbed layer form. Chemisorbed layer can be thermally desorbed only. Hence in the decreasing cycle of %RH, the initially adsorbed water is not removed fully leading to hysteresis. The value of hysteresis for sensing element W is .47% at annealing temperature 600°C which is less for highest temperature .

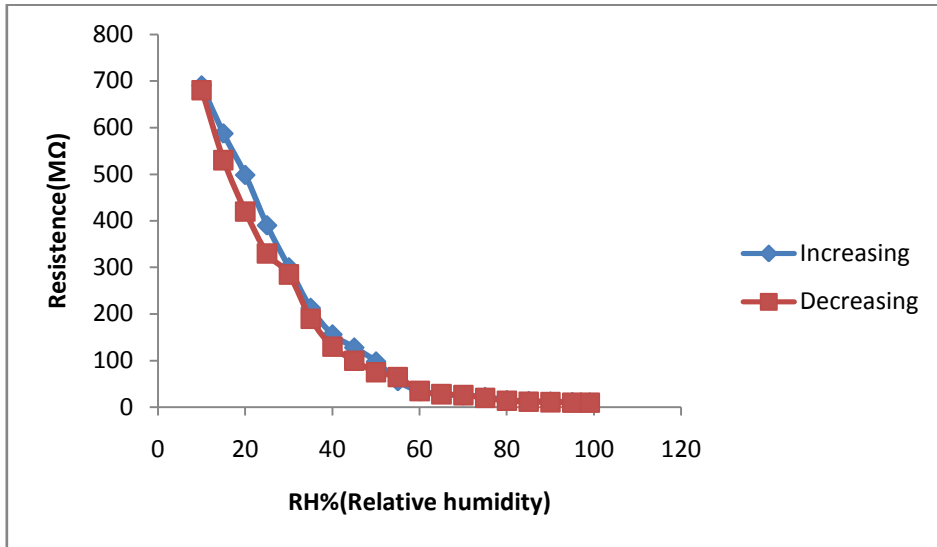


Fig. 05: Hysteresis graph for the sensing element Pure WO₃ annealed at 300°C

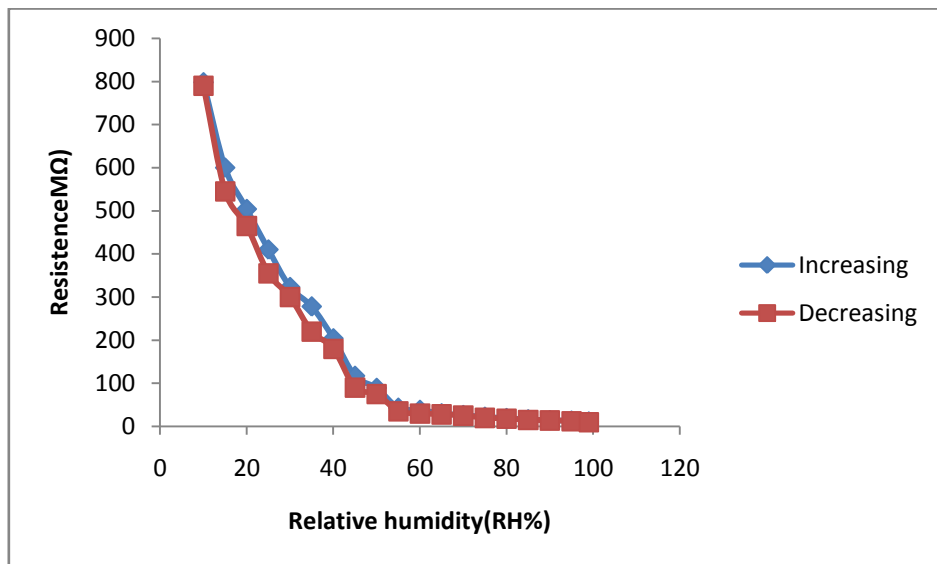


Fig. 06: Hysteresis graph for the sensing element Pure WO₃ annealed at 400°C

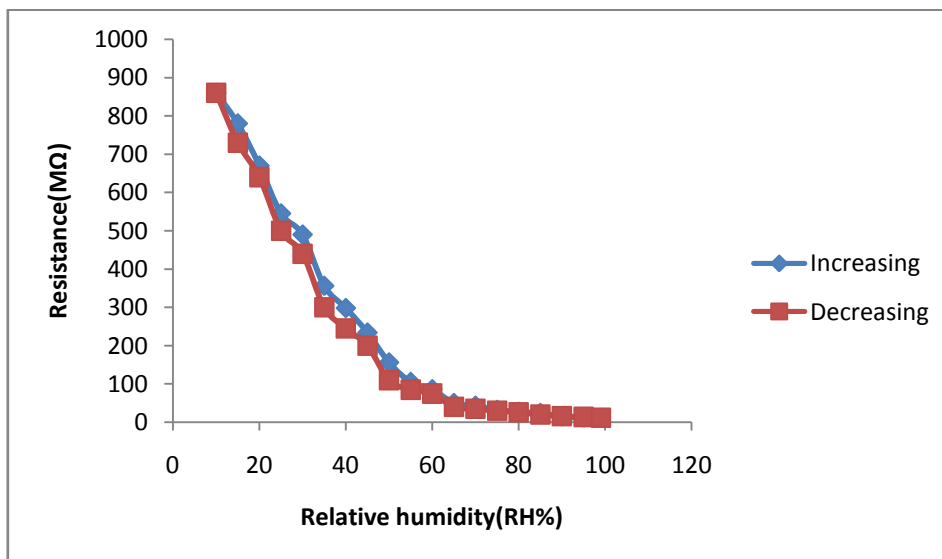


Fig. 07: Hysteresis graph for the sensing element Pure WO₃ annealed at 500°C

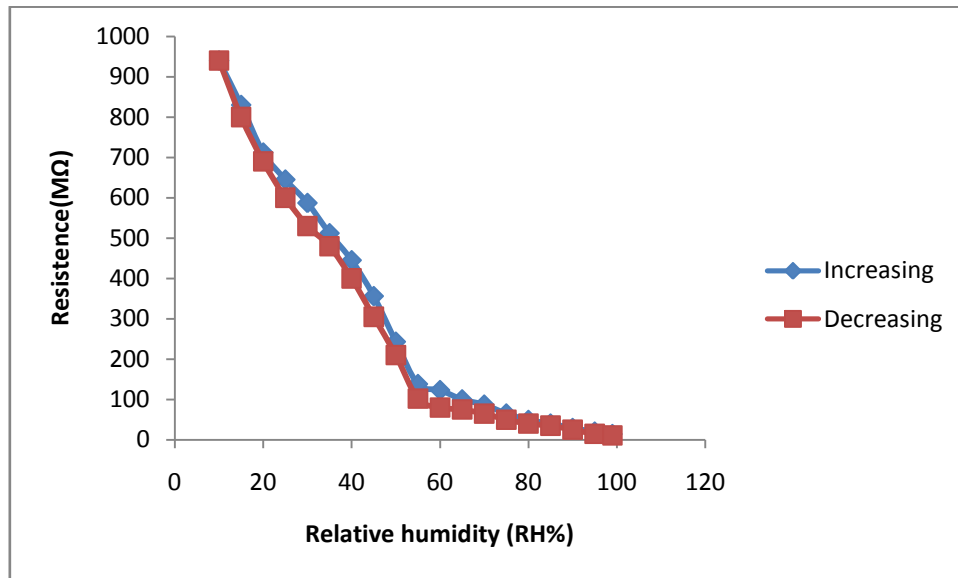


Fig. 08: Hysteresis graph for the sensing element Pure WO_3 annealed at $600^\circ C$

4-Ageing effect: The sensing properties of the samples W at annealing temp. 300 to $600^\circ C$ have been examined again in the humidity control chamber after six months and variation of resistance with %RH recorded. The variation of resistance of sensing elements WO_3 with change in %RH after six months have been shown in fig 09,10,11 and 12 for annealing temperatures $300^\circ C$, $400^\circ C$, $500^\circ C$ and $600^\circ C$ respectively. In this figures the value of average sensitivity in the range 10% to 99% RH of pure WO_3 at $600^\circ C$ is $10.40 M\Omega\%RH$ and after six months is $8.87 M\Omega\%RH$ which are highest remaining to all temperatures, which is shown in table 2. Fig.(13) shows the combined ageing graphs and fig.(14) shows the sensitivity graph for ageing effect .Fig(15) shows the sensitivity comparison graphs for both humidification and ageing samples.

Result shows that the sensitivity less decrease with the time period and samples have less effect of ageing and low hysteresis.

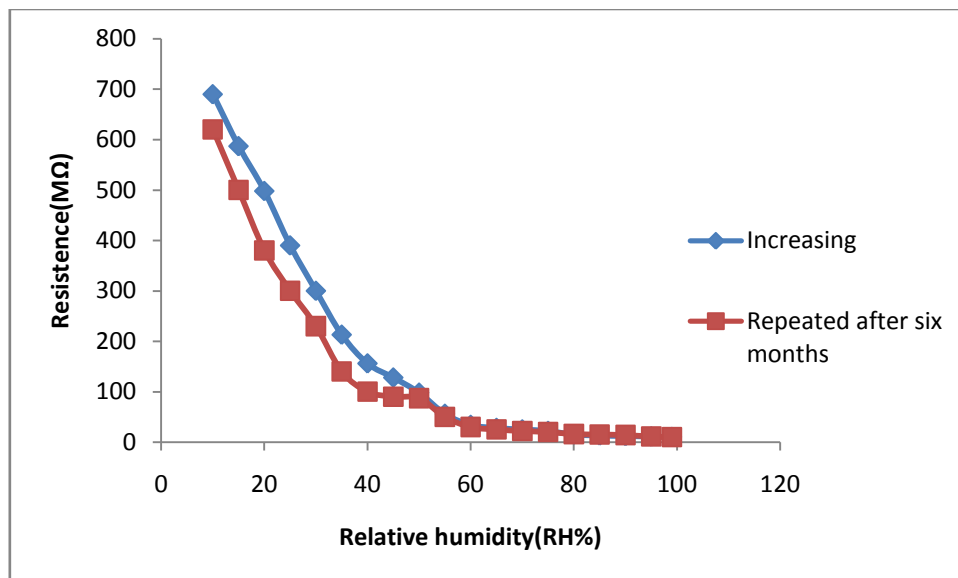


Fig. 09: Variations in Resistance with % RH for Sample Pure WO_3 annealed at $300^\circ C$ (After Six months)

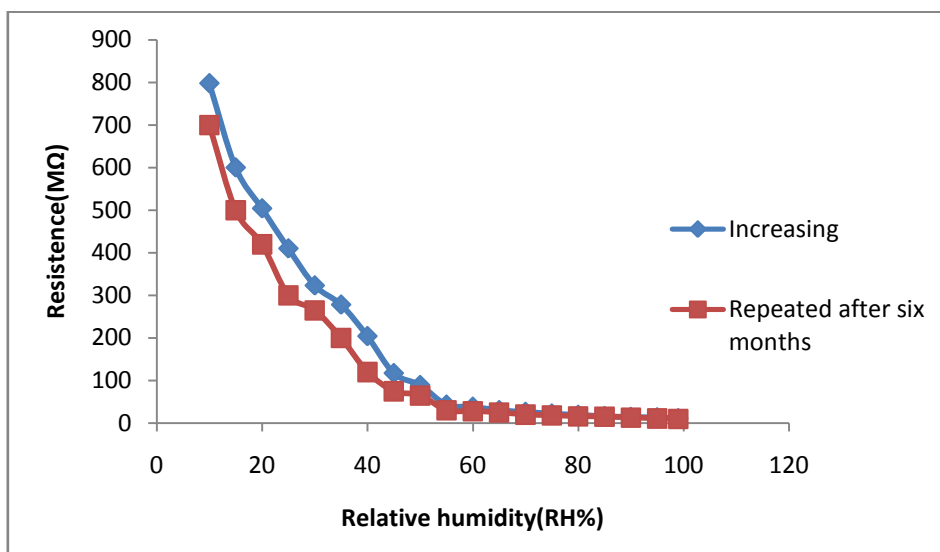


Fig. 10: Variations in Resistance with % RH for Sample Pure WO_3 annealed at $400^\circ C$ (After Six months)

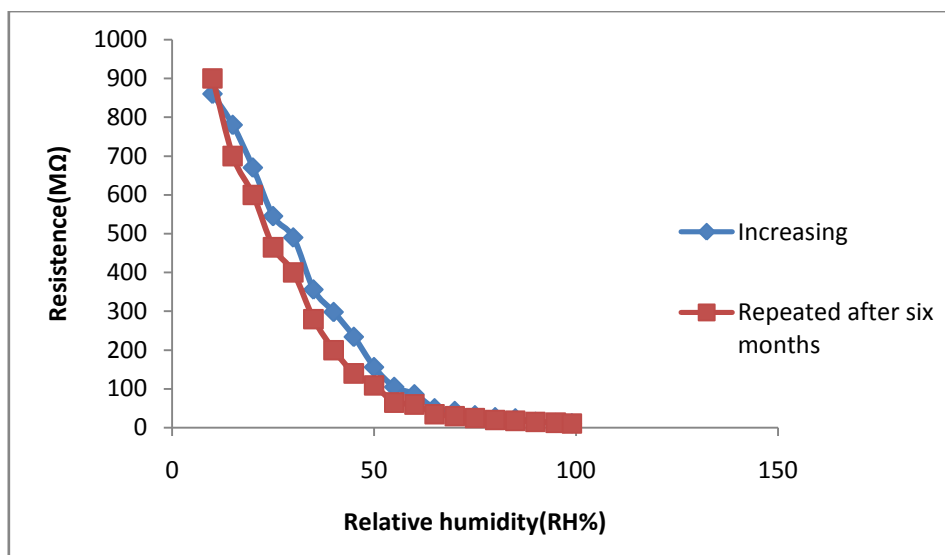


Fig. 11: Variations in Resistance with % RH for Sample Pure WO_3 annealed at $500^\circ C$ (After Six months)

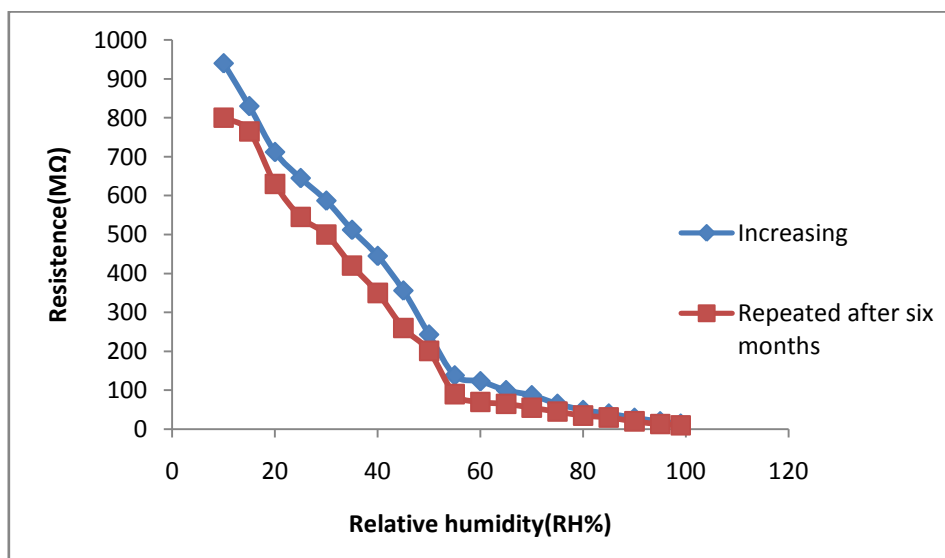


Fig. 12: Variations in Resistance with % RH for Sample Pure WO_3 annealed at $600^\circ C$ (After Six months)

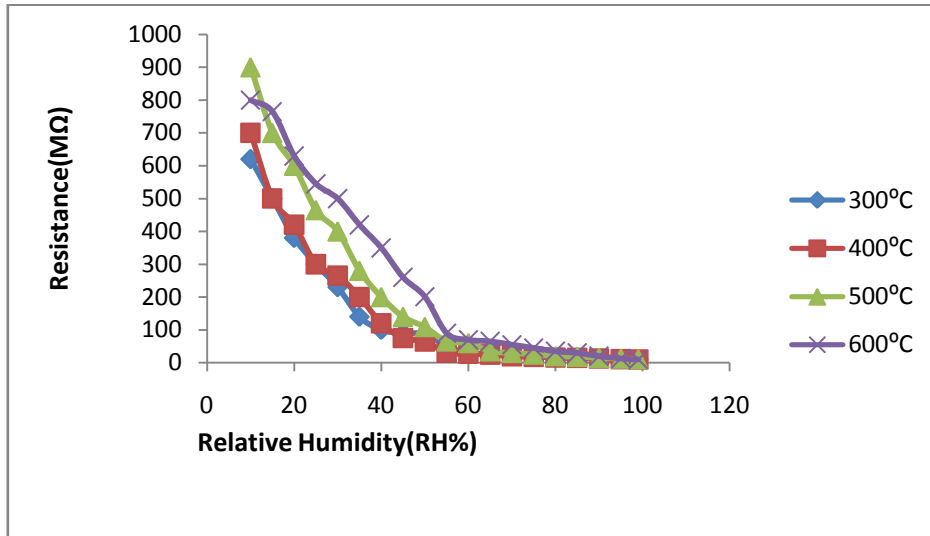


Fig.13: Variations in Resistance with % RH for Sample Pure WO₃ annealing temperature at 300°C to 600°C(Ageing Graph)

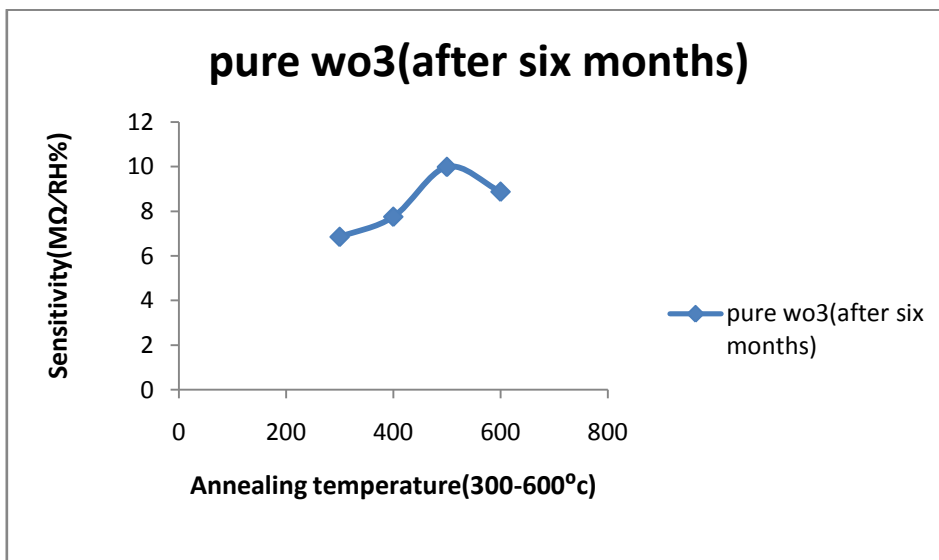


Fig.14: Sensitivity graph for pure wo3 (after six months)

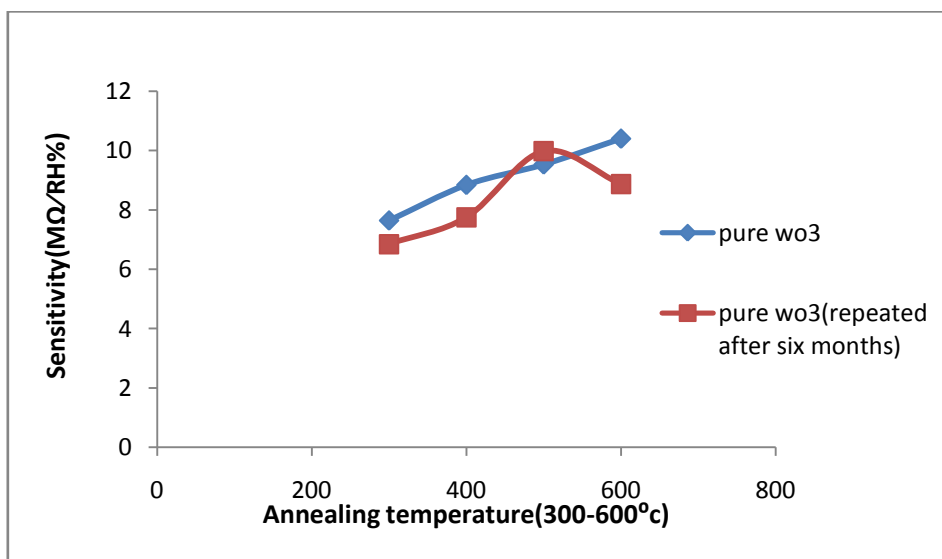


Fig.15: Sensitivity Comparison graph for humidification and Ageing cycle pure wo3 (after six months)

Characterization: (1)-scanning electron micrograph: Surface morphology of sensing element has been studied using scanning electron microscope unit (SEM, leo-0430, and Cambridge). The pure WO_3 sample at annealing temperature 600°C has a best sensitivity, low hysteresis, less effect of ageing and high reproducibility. FIG.(16),(17),(18),(19), shows scanning electron micrograph of pure WO_3 at annealing temperatures 300°C , 400°C , 500°C and 600°C respectively. SEM shows that molecules of WO_3 particles form flakes and lots of pores. These pores are expected to provide sites for humidity adsorption. SEM reveals that the surface morphology is characterized by typical porous structure and small crystallites without inside pores but many inter grain pores. The grain size of pure WO_3 at annealing temperatures 300°C , 400°C , 500°C and 600°C are 114nm , 135nm , 148nm and 158nm respectively.

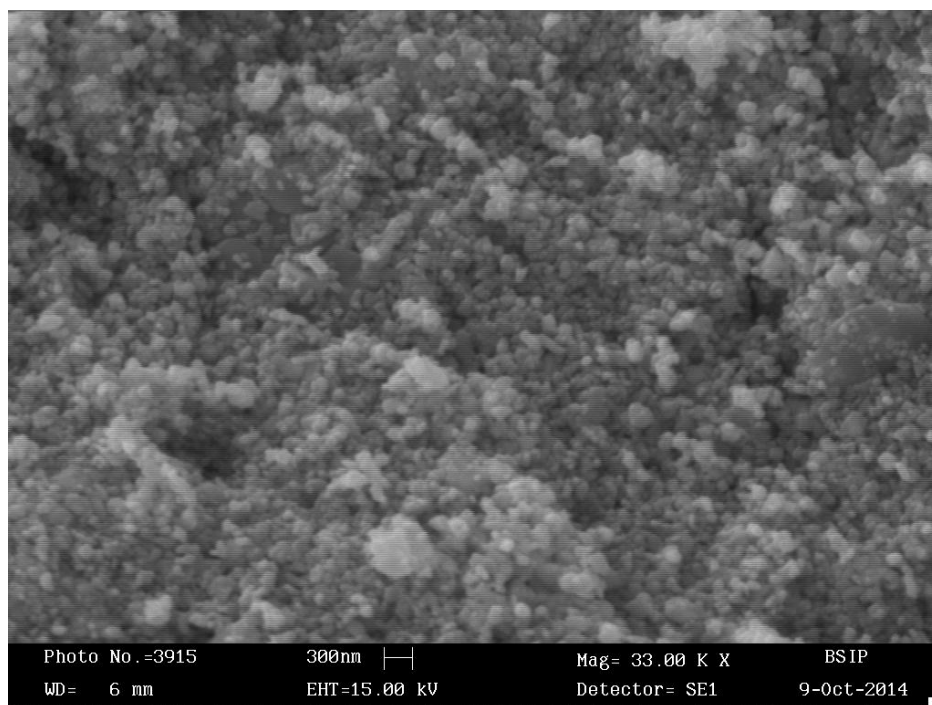


Fig. 16: SEM Micrograph of Sensing Element Pure WO_3 annealed at 300°C

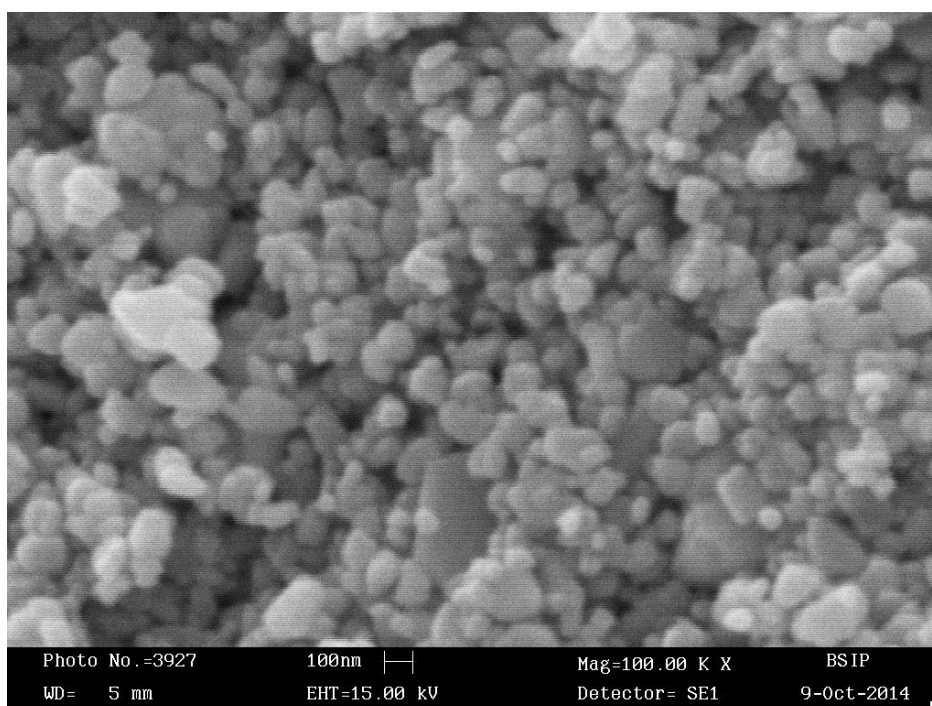


Fig. 17: SEM Micrograph of Sensing Element Pure WO_3 annealed at 400°C

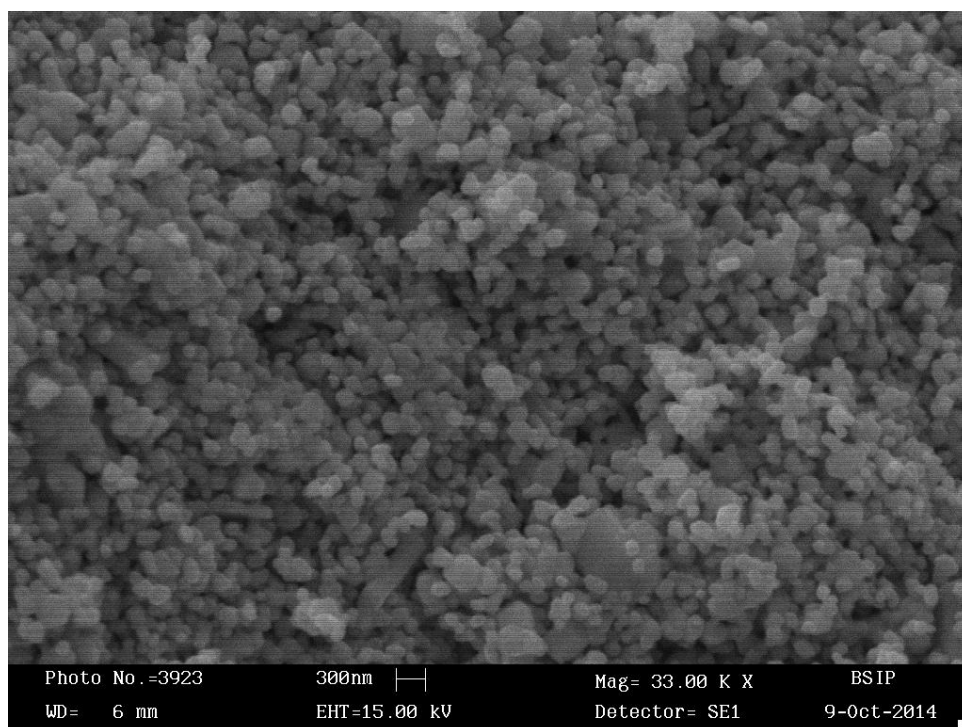


Fig. 18: SEM Micrograph of Sensing Element Pure WO_3 annealed at 500°C

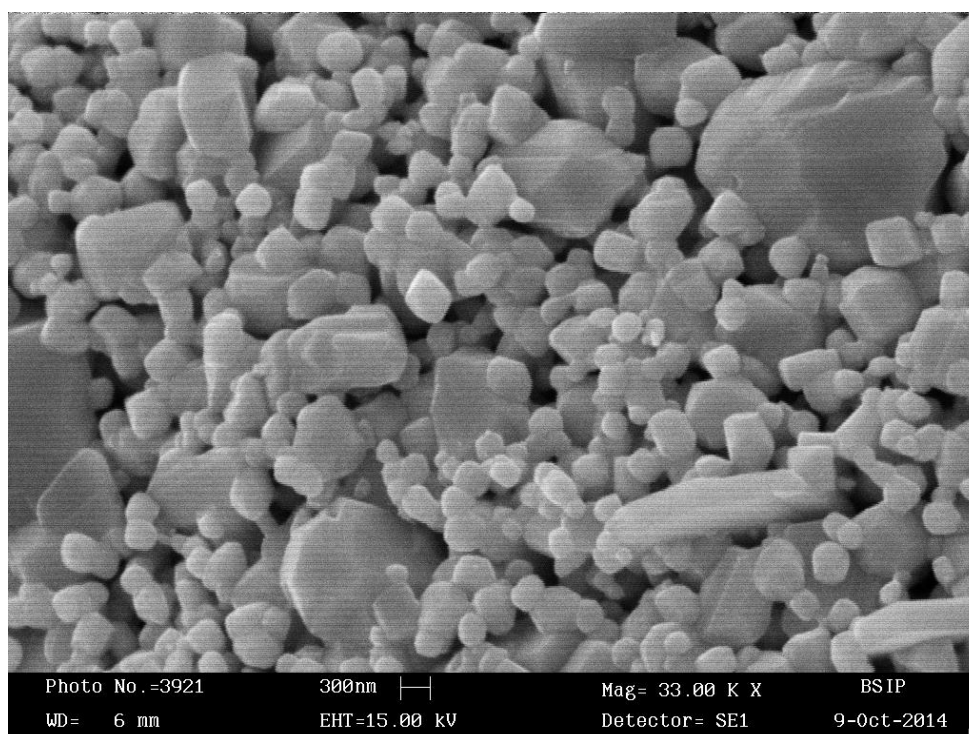


Fig. 19: SEM Micrograph of Sensing Element Pure WO_3 annealed at 600°C

(2)-X-Ray diffraction analysis: X-ray diffraction has been studied using XPERT PRO – Analytical XRD system (Netherlands). The wavelength of the $CuK\alpha$ source used is 1.54060 \AA . Fig.(20) shows X-ray pattern for the sensing elements (W) at annealing temp 600°C prepared at room temp. The average crystallite size of the samples has been calculated using Debye Scherer's formula $D = K\lambda / \beta \cos\theta$ where D is the crystallite size, K is the fixed number of 0.9, λ is the X-ray wavelength, θ is the Bragg angle and β is the full width at half maximum of the peak, the crystallite size calculated from Scherer's formula for the sample pure WO_3 at annealing temp. 600°C is found to be 72.4 nm.

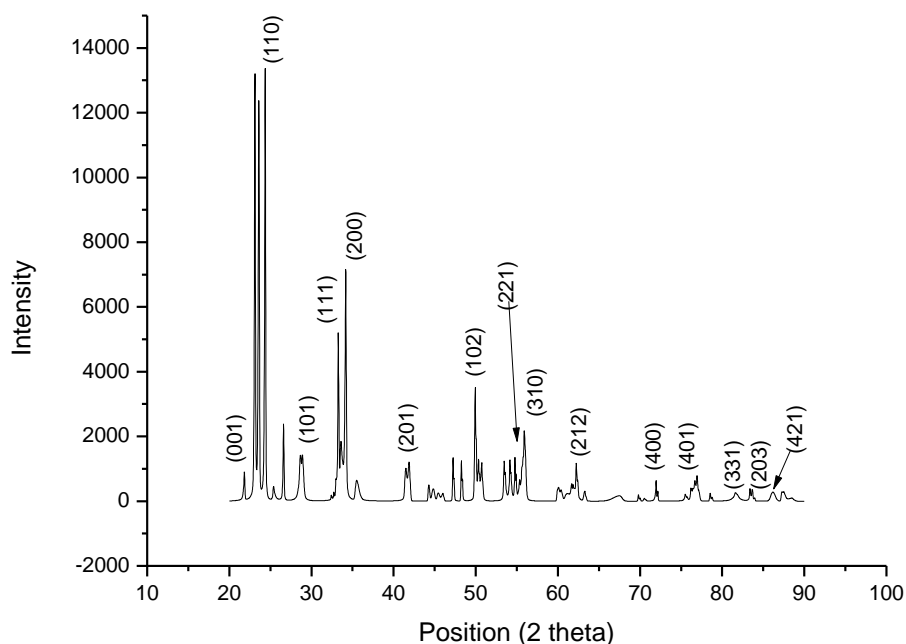


Fig.20: XRD pattern for sample pure WO_3

III. Conclusion

The comparative studies of all samples of WO_3 shows that the average sensitivity of WO_3 at annealing temperature $600^\circ C$ are $10.40M\Omega\%RH$ which is highest in comparison to all temperatures. . Now wo_3 shows best sensitivity, low hysteresis, less effect of ageing and higher reproducibility at annealing temp $600^\circ c$. The grain size of wo_3 at annealing temperature $600^\circ C$ is 158 nm and crystallite size is 72.4 nm its shape is tetragonal.

Acknowledgements

The author would like to thanks The Birbal Sahni, Lucknow university, Lucknow and Physics department, Lucknow university, Lucknow, for providing SEM and XRD respectively.

References

- [1]. Aihua Yana, Changsheng Xie, Dawen Zeng, Shuizhou Cai, Huayao Li Journal of Alloys and Compounds 495 (2010) 88–92.
- [2]. P.-G. Su a , Wu Ren-Jang b , Nieh Fang-Pei c , Talanta 59 (2003) 667-672.
- [3]. Liang Zhou , Qijun Ren , Xufeng Zhou , Jiawei Tang , Zhanghai Chen .Chengzhong Microporous and Mesoporous Materials 109 (2008) 248–257.
- [4].] Zhifu Liu, Masashio Miyauchi, Toshinari Yamazaki, Yanbai Shen, Sensors and Actuators B 140 (2009) 514–519.
- [5]. Sun, M., Xu, N., Cao, Y.W., Yao, J.N. and Wang, E.G., J. Mater Res., 15: 927 (2000).
- [6]. Guo, J.D. and Hagen, G., Sol. Energy Mat. Sol. Cells, 58: 277 (1999).
- [7]. Granqvist, C.G., Sol. Energy Mat. Sol. Cells, 60: 201 (2000).
- [8]. Llobet, E., Molas, G., Molinas, P., Calderer, J., Vilanova, X., Brezmes, J. and Sueiras., J. Electrochem. Soc., 147: 776 (2000).
- [9]. Chandra. S.R., Govindraj, A. and Rao, C.N.R., J. Mater. Chem., 16: 3936 (2006).
- [10]. S. Luo, G. Fu, H. Chen and Y. Zhang, Materials Chemistry and Physics 109 (2008) 541.
- [11]. A.A. Tomchenko, V.V. Khatko and I.L. Emelianov, Sensors and Actuators B 46 (1998) 8.
- [12]. A. Hoel, L.F. Reyes, P. Heszler, V. Lantto, C.G. Granqvist, Current Applied Physics, 4 (2004) 547.
- [13]. C. Matei Ghimbeu, M. Lumberras, M. Siadat, J. Schoonman, Materials Science in Semiconductor Processing, 13 1.
- [14]. E. Rossinyol, A. Prim, E. Pellicer J. Rodrigues, F. Peiro, A. Cornet, J.R. Morante, B. Tian, T. Bo and D. Zhao, Sensors and Actuators B 126 (2007) 18.
- [15]. E. Comini, L. Pandolfi, S. Kaciulis, G. Faglia and G. Sberveglieri, Sensors and Actuators B 127 (2007) 28.
- [16]. G. Korotcenkov, V. Brinzari, A. Cerneavshi, M. Ivanov, V. Golovanov, A. Cornet, J. Morante, A. Cabot and Arbiol, Thin Solid Films, 460 (2004) 315.
- [17]. A. Rothschild and Y. Komem, J. Appl. Phys. 95 (2004) 6374.
- [18]. A. Cremonesi, Y. Djaoued, D. Bersani and Lottici P.P., Thin Solid Films 516 (2008) 4128.
- [19]. X. Shen, G. Wang, D. Wexler, Sensors and Actuators B: Chemical, 143 (2009) 325.